Theor Chem Acc (2003) 110: 377–386
DOI 10.1007/s00214-003-0491-x

Theoretical
Chemistry Accounts

Regular article

Theoretical study of the gas-phase thermolysis reaction of alkyl (ethyl, isopropyl, and *tert*-butyl) *N*,*N*-dimethylcarbamates and *N*,*N*-diethylcarbamates

Camilo Quijano[1], **Rafael Notario**[2], **Jairo Quijano**[1], **Claudia Sánchez**[1], **LuisA. León**[1], **Ederley Vélez**[1]

[1] Laboratorio de Fisicoquímica Orgánica, Facultad de Ciencias, Universidad Nacional de Colombia, Sede Medellín, Apartado Aéreo 3840, Medellín, Colombia
[2] Instituto de Química Física "Rocasolano", C.S.I.C., Serrano 119, 28006, Madrid, Spain

Received: 5 September 2002 / Accepted: 30 May 2003 / Published online: 25 November 2003

Abstract. Theoretical studies on the thermolysis in the gas phase of alkyl *N*,*N*-dialkylcarbamates were carried out using ab initio theoretical methods, at the MP2/6-31G(d), MP2/6-31++G(d,p) and MP2/6-311++G(2d,p)//MP2/6-31G(d) levels. The reactions have two steps: the first one corresponds to the formation of an alkene and a neutral dialkylcarbamic acid intermediate via a six-membered cyclic transition state; the second one is the decarboxylation of this intermediate via a four-membered cyclic transition state, leading to carbon dioxide and the corresponding dialkylamine. The progress of the reactions was followed by means of the Wiberg bond indices. The results indicate that the transition states have character intermediate between reactants and products, and the calculated synchronicities show that the reactions are slightly asynchronous. The bond-breaking processes are more advanced than the bond-forming ones, indicating a bond deficiency in the transition states. The rate constants calculated for all the reactions agree very well with the available experimental data.

Keywords: Alkyl *N*,*N*-dialkylcarbamates – Thermal decomposition – Ab initio computational methods – Reaction mechanism – Transition-state structure

Introduction

The first homogeneous, unimolecular thermal decomposition of a carbamate in the gas phase was reported by Daly and Ziolkowski [1]. They studied the decomposition of ethyl *N*-methyl-*N*-phenylcarbamate that leads to *N*-methylaniline, ethylene, and carbon dioxide. The generally accepted mechanism of this elimination process consisted of a six-membered cyclic transition state (TS) similar to those described for acetates, carbonates, and xanthates [1, 2, 3, 4].

Daly and Ziolkowski [5] also studied the pyrolysis reaction of methyl *N*-methylcarbamate. The results showed that its decomposition process differs from that of ethyl *N*-methyl-*N*-phenylcarbamate, the reaction being

$$CH_3NHCOOCH_3 \rightarrow CH_3NCO + CH_3OH. \qquad (1)$$

The presence of a hydrogen atom at the nitrogen atom was believed to be responsible for the different mechanistic pathway, and the elimination reaction was explained in terms of a four-membered cyclic TS mechanism.

In this work we have carried out a theoretical study on the gas-phase thermolysis reaction of six alkyl esters of *N*,*N*-dialkylcarbamic acids: ethyl *N*,*N*-dimethylcarbamate, I, isopropyl *N*,*N*-dimethylcarbamate, II, *tert*-butyl *N*,*N*-dimethylcarbamate, III, ethyl *N*,*N*-diethylcarbamate, IV, isopropyl *N*,*N*-diethylcarbamate, V, and *tert*-butyl *N*,*N*-diethylcarbamate, VI (see Fig. 1).

The thermolysis reactions of these *N*,*N*-dimethylcarbamates [6, 7] and *N*,*N*-diethylcarbamates [8] have been previously studied. The experimental results [6, 7, 8]

From the Proceedings of the 28th Congreso de Químicos Teóricos de Expresión Latina (QUITEL 2002)

Correspondence to: R. Notario
e-mail: rnotario@iqfr.csic.es

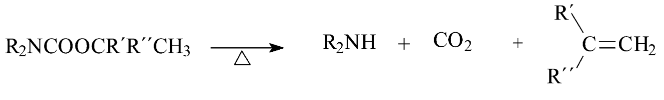

$$R_2NCOOCR'R''CH_3 \xrightarrow[\triangle]{} R_2NH + CO_2 + \overset{R'}{\underset{R''}{C}}{=}CH_2$$

I $R = CH_3$; $R', R'' = H$

II $R, R' = CH_3$; $R'' = H$

III $R, R', R'' = CH_3$

IV $R = CH_2CH_3$; $R', R'' = H$

V $R = CH_2CH_3$; $R' = CH_3$; $R'' = H$

VI $R = CH_2CH_3$; $R', R'' = CH_3$

Fig. 1. Thermolysis reaction of alkyl *N,N*-dialkylcarbamates

proved the reactions to be homogeneous, unimolecular, and to obey a first-order rate law. The decomposition of these carbamates leads to the formation of the corresponding dialkylcarbamic acid and an alkene as expected by a molecular cis elimination [9]. However, the neutral carbamic acid intermediates, under the experimental conditions (17–160 Torr, 220–400 °C), undergo a decarboxylation process, leading to CO_2 and the corresponding dialkylamine as shown in Fig. 1. The available experimental kinetic parameters are listed in Table 1.

The mechanism suggested from the experiments [6, 7, 8] for the decomposition process for these types of compounds is described in Fig. 2. The products of the reactions suggested that the process should be via a six-membered cyclic TS for the first step and via a four-membered cyclic TS for the second one.

The aim of this work is to carry out a computational study in order to explore the nature of the reaction mechanism for the unimolecular decomposition of the alkyl *N,N*-dialkylcarbamates studied in the gas phase. To our knowledge, this is the first theoretical study on the thermolysis reaction of these types of compounds.

Computational details

All the calculations were carried out using the Gaussian98 computational package [10]. The geometric parameters for all the reactants, the TSs, and the products of the reactions studied were fully optimized using ab initio analytical gradients at the MP2 level [11] with the 6-31G(d) basis set [12]. Each stationary structure was characterized as a minimum or a saddle point of first order by analytical frequency calculations. A scaling factor [13] of 0.9670 for the zero-point vibrational energies was used. Thermal corrections to enthalpy and entropy values were evaluated at the experimental temperature of 593.15 K. To calculate enthalpy and entropy values at a temperature *T*, the difference between the values at that temperature and 0 K was evaluated according to standard thermodynamics [14].

Intrinsic reaction coordinate (IRC) calculations [15] were performed in all cases to verify that the localized TS structures connect with the corresponding minimum stationary points associated with reactants and products.

Owing to the nature of the TS of the reactions studied, involving bond breaking, we reoptimized the geometries of all the reactants, TS, and products of the reactions, at the higher MP2/6-31++G(d,p) level [16]. Also, single-point energy calculations at the MP2/6-311++G(2d,p) level were performed on the MP2/6-31G(d) optimized structures.

The bonding characteristics of the different reactants, TS, and products were investigated using a population partition technique, the natural bond orbital (NBO) analysis of Reed and Weinhold [17, 18]. The NBO formalism provides values for the atomic natural total charges and also provides the Wiberg bond indices [19] used to follow the progress of the reactions. The NBO analysis was performed using the NBO program [20], implemented in the Gaussian98 package [10], and was carried out on the MP2 charge densities in order to explicitly include electron correlation effects.

Table 1. Experimental kinetic parameters obtained for the thermolysis reaction of the *N,N*-dimethylcarbamates and *N,N*-diethylcarbamates studied, at 593.15 K

Reaction	10^4k (s^{-1})	log*A*	E_a (kJ mol^{-1})	Reference
$(CH_3)_2NCOOCH_2CH_3$, I	0.58	12.10	185.5	[6]
$(CH_3)_2NCOOCH(CH_3)_2$, II	12.02	13.04	181.2	[6]
$(CH_3)_2NCOOC(CH_3)_3$, III	912.0	12.87	157.9	[6]
	782.2	13.27	163.2	[7]
$(CH_3CH_2)_2NCOOCH_2CH_3$, IV	0.56	11.47 ± 0.25	178.4 ± 3.1	[8]
$(CH_3CH_2)_2NCOOCH(CH_3)_2$, V	9.77	12.83 ± 0.70	179.8 ± 7.9	[8]
$(CH_3CH_2)_2NCOOC(CH_3)_3$, VI	794.3	12.87 ± 0.62	158.6 ± 6.2	[8]

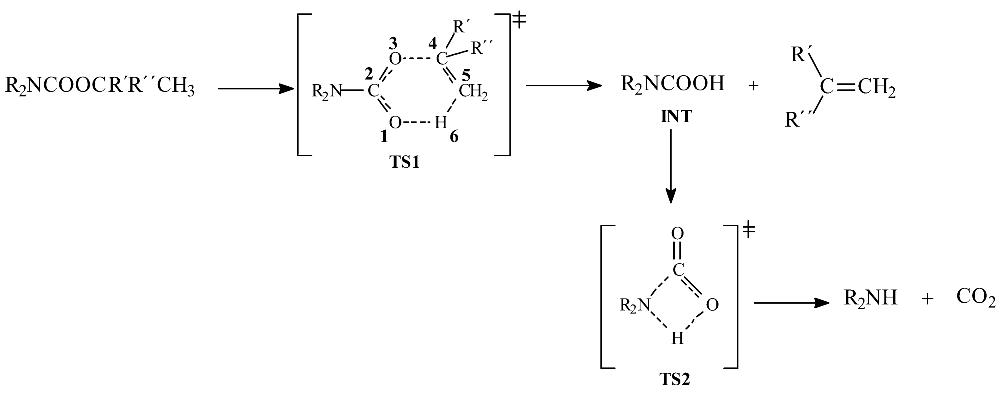

Fig. 2. Mechanism proposed from experiments for the thermolysis reaction of alkyl *N,N*–dialkylcarbamates

We selected the classical TS theory (TST) [21, 22] to calculate the kinetic parameters. The rate constant, $k(T)$, for each elementary step of the kinetic scheme (Fig. 2) was computed using this theory assuming that the transmission coefficient is equal to unity, as expressed by the following relation:

$$k(T) = \frac{k_B T}{h} \exp\left[\frac{-\Delta G^{\neq}(T)}{RT}\right], \tag{2}$$

where k_B, h, and R are the Boltzmann constant, the Planck constant, and the universal gas constant, respectively. $\Delta G^{\neq}(T)$ is the standard-state free energy of activation, at the absolute temperature T.

The activation energies, E_a, and the Arrhenius A factors were calculated using Eqs. (3) and (4), respectively, derived from the TST theory:

$$E_a = \Delta H^{\neq}(T) + RT, \tag{3}$$

$$A = \frac{e k_B T}{h} \exp\left[\frac{\Delta S^{\neq}(T)}{R}\right]. \tag{4}$$

Results and discussion

Electronic energies, evaluated at the MP2/6-31G(d), MP2/6-31++G(d,p), and MP2/6-311++G(2d,p)//MP2/6-31G(d) levels of theory, and zero-point vibrational energies, thermal correction to enthalpies and entropies, obtained at the MP2/6-31G(d) level, for all the reactants, TSs, and products involved in the six reactions studied are collected in Table 2.

The pathway (Fig. 2) describes a two-step mechanism. The first step is a process in which an alkene and a dialkylcarbamic acid intermediate are formed via a six-membered cyclic TS, TS1, where the hydrogen atom of the CH_3 group is migrating to the oxygen atom of the carbonyl group. The second step is the decarboxylation process of the neutral dialkylcarbamic acid intermediate, via a four-membered cyclic TS, TS2, leading to CO_2 and the corresponding dialkylamine.

Free-energy reaction profiles, obtained at the MP2/6-311++G(2d,p)//MP2/6-31G(d) level of theory, for the decomposition processes of the alkyl *N*,*N*-dimethylcarbamates and alkyl *N*,*N*-diethylcarbamates studied are presented in Figs. 3 and 4, respectively.

On the basis of the results reported here, it is clear that the first step of the processes is the rate-determining step, whereas the decarboxylation of the corresponding carbamic acid intermediate via a four-membered cyclic TS (TS2-Me or TS2-Et) is a rapider process with smaller activation energy. The calculated activation free energies for the first reaction step are 191.1, 183.8, and 161.3 kJ mol^{-1}, for reactionsI, II, and III, respectively, and 193.9, 186.1, and 162.7 kJ mol^{-1}, for reactions IV, V, and VI, respectively. The activation free energies for the second reaction step, via TS2 TSs, are only 149.7, and 142.3 kJ mol^{-1}, for the decarboxylation of dimethylcarbamic acid (reactions I, II, and III) and diethylcarbamic acid (reactions IV, V, and VI), respectively. The overall processes are exergonic, with reaction free energies of −105.3, −108.6, and −116.6 kJ mol^{-1}, for reactions I, II, and III, respectively, and of −106.3, −109.2, and −117.3 kJ mol^{-1}, for reactions IV, V, and VI, respectively.

Our calculations for the reactions in Fig. 2 indicate that all the reactions have very similar concerted processes with a hydrogen at the alkyl moiety of the

Table 2. Electronic energies, evaluated at the MP2/6-31G(d), MP2/6-31++G(d,p), and MP2/6-311++G(2d,p)//MP2/6-31G(d) levels, zero-point vibrational energies (*ZPE*) and thermal corrections to enthalpies (*TCH*) in hartrees, and entropies, *S*, (J mol^{-1} K^{-1}), for all the reactants, transition states, and products involved in the reactions studied

Species	MP2/6-31G(d)	MP2/6+31++G(d,p)	MP2/6-311++G(2d,p)//MP2/6-31G(d)	ZPE[a]	TCH[a]	*S*[a]
I	−401.101737	−401.213483	−401.446862	0.168669	0.201390	533.13
TS1-I	−401.011301	−401.129804	−401.365897	0.161152	0.193862	537.15
$(CH_3)_2NCOOH$	−322.776886	−322.858317	−323.054964	0.110223	0.133832	436.73
$CH_2=CH_2$	−78.285027	−78.323549	−78.361792	0.052053	0.062277	256.06
TS2-Me	−322.716348	−322.799190	−322.995749	0.105358	0.127785	420.45
$(CH_3)_2NH$	−134.665298	−134.733202	−134.804683	0.095249	0.110436	328.60
CO_2	−188.107747	−188.117959	−188.245426	0.011510	0.019938	243.49
II	−440.274171	−440.403947	−440.656270	0.197182	0.234816	581.24
TS1-II	−440.187076	−440.323151	−440.578282	0.189862	0.227414	584.84
$CH_3CH=CH_2$	−117.455545	−117.511373	−117.569035	0.081581	0.096090	320.91
III	−479.443584	−479.591278	−479.862688	0.225537	0.268136	624.52
TS1-III	−479.362979	−479.516883	−479.791208	0.218215	0.260849	637.70
$(CH_3)_2C=CH_2$	−156.627342	−156.700659	−156.778367	0.110599	0.129761	366.18
IV	−479.440805	−479.588056	−479.859574	0.227435	0.269073	625.66
TS1-IV	−479.350366	−479.504454	−479.778516	0.220064	0.261583	625.51
$(CH_3CH_2)_2NCOOH$	−401.115625	−401.232664	−401.467428	0.169072	0.201509	527.35
TS2-Et	−401.056975	−401.175235	−401.410070	0.163921	0.195430	515.10
$(CH_3CH_2)_2NH$	−213.002780	−213.106580	−213.215769	0.153765	0.177974	429.33
V	−518.613403	−518.778672	−519.069123	0.255935	0.302495	673.67
TS1-V	−518.526054	−518.697678	−518.990768	0.248733	0.295146	675.26
VI	−557.783098	−557.966300	−558.275815	0.284319	0.335818	715.67
TS1-VI	−557.702127	−557.891521	−558.203839	0.277076	0.328575	728.89

[a] Obtained at the MP2/6-31G(d) level

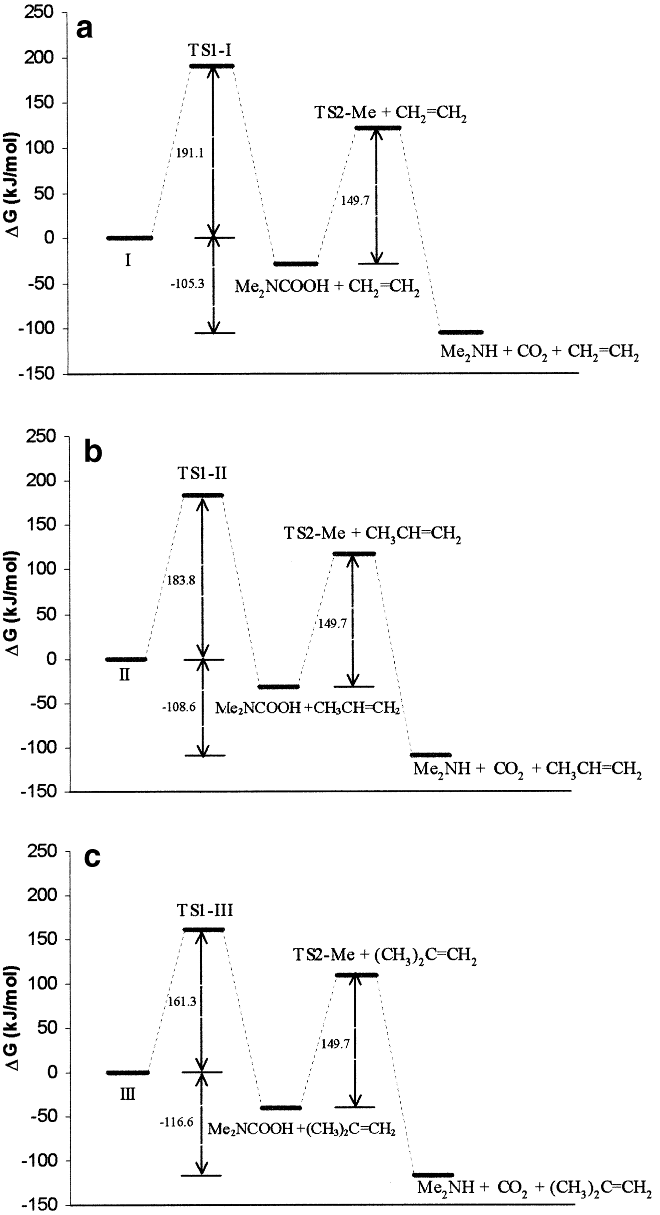

Fig. 3a–c. Free-energy profiles at 593.15 K, evaluated at the MP2/6-311++G(2d,p)//6-31 G(d) level for the thermolysis reaction of alkyl *N,N*-dimethylcarbamates. **a** Relative free energy values (to reactant I) of the stationary points found are as follows: **TS1-I** 191.1; $Me_2NCOOH + CH_2{=}CH_2$ −29.0; TS2-Me + $CH_2{=}CH_2$ 120.7; $Me_2NH + CO_2 + CH_2{=}CH_2$ −105.3. **b** Relative free energy values (to reactant II) of the stationary points found are as follows: TS1-II 183.8; $Me_2NCOOH + CH_3CH{=}CH_2$ −32.3; TS2-Me + $CH_3CH{=}CH_2$ 117.4; $Me_2NH + CO_2 + CH_3CH{=}CH_2$ −108.6. **c** Relative free energy values (to reactant III) of the stationary points found are as follows: TS1-III 161.3; $Me_2N\text{-}COOH + (CH_3)_2C{=}CH_2$ −40,3; TS2-Me + $(CH3)_2C{=}CH_2$ 109.4; $Me_2NH + CO_2 + (CH_3)_2C{=}CH_2$ −116.6

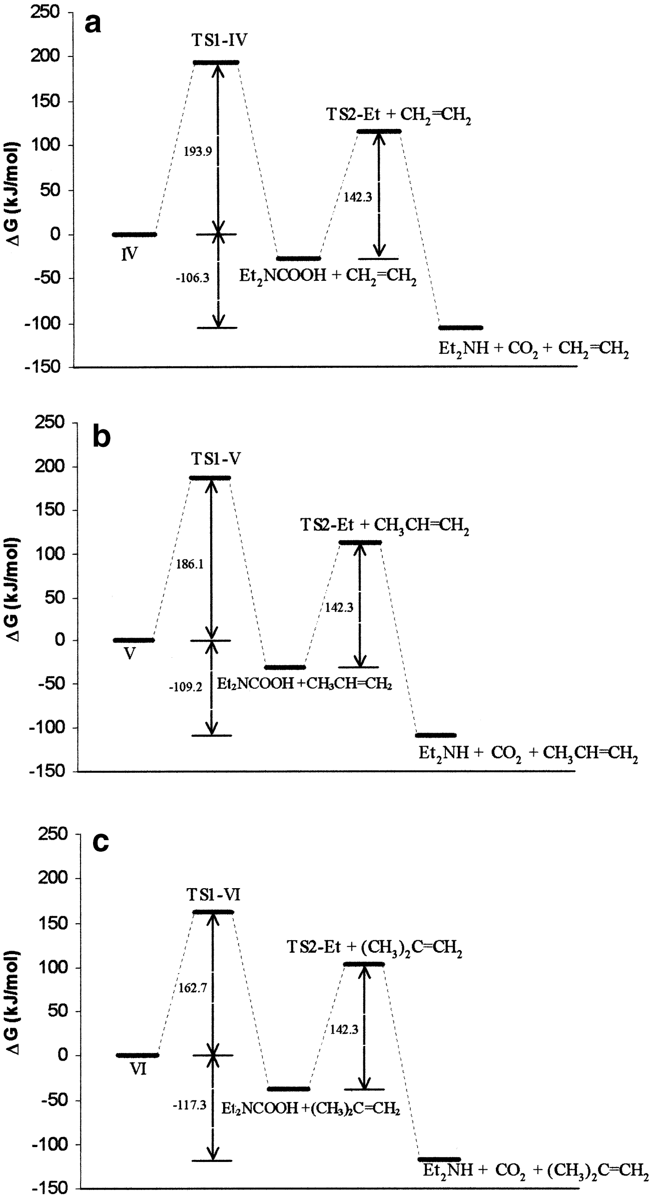

Fig. 4a–c. Free-energy profiles at 593.15 K, evaluated at the MP2/6-311++G(2d,p)//6-31 G(d) level, for the thermolysis reaction of alkyl *N,N*-diethylcarbamates. **a** Relative free energy values (to reactant IV) of the stationary points found are as follows: TS1-IV 193,9; $Et_2NCOOH + CH_2{=}CH_2$ −27.2; TS2-Et + $CH_2{=}CH_2$ 115.1; $Et_2NH + CO_2 + CH_2{=}CH_2$ −106.3. **b** Relative free energy values (to reactant V) of the stationary points found are as follows: TS1-V 186.1; $Et_2NCOOH + CH_3CH{=}CH_2$ −30.2; TS2-Et + $CH_3CH{=}CH_2$ 112,1; $Et_2NH + CO_2 + CH_3CH{=}CH_2$ −109.2. **c** Relative free energy values (to reactant VI) of the stationary points found are as follows: TS1-VI 162.7; $Et_2N\text{-}COOH + (CH_3)_2C{=}CH_2$ −38.2; TS2-Et + $(CH_3)_2C{=}CH_2$ 104.1; $Et_2NH + CO_2 + (CH_3)_2C{=}CH_2$ −117.3

ester transferring and a C–O bond breaking via a six-membered cyclic TS (molecular cis elimination) for the first step.

There is one and only one imaginary vibrational frequency in the TSs optimized. In the case of those corresponding to the first step of the elimination reactions studied they are 1,635.3*i*, 1,561.1*i*, 1,495.2*i*, 1,636.2*i*, 1,567.7*i*, and 1,509.1*i* cm^{-1} for TS1-I, TS1-II, TS1-III, TS1-IV, TS1-V, and TS1-VI, respectively, evaluated at the MP2/6-31G(d) level of theory. For the TSs of the second step of the reactions, TS2-Me and TS2-Et, the imaginary frequencies are 1,696.9*i*, and 1,694.2*i* cm^{-1}, respectively.

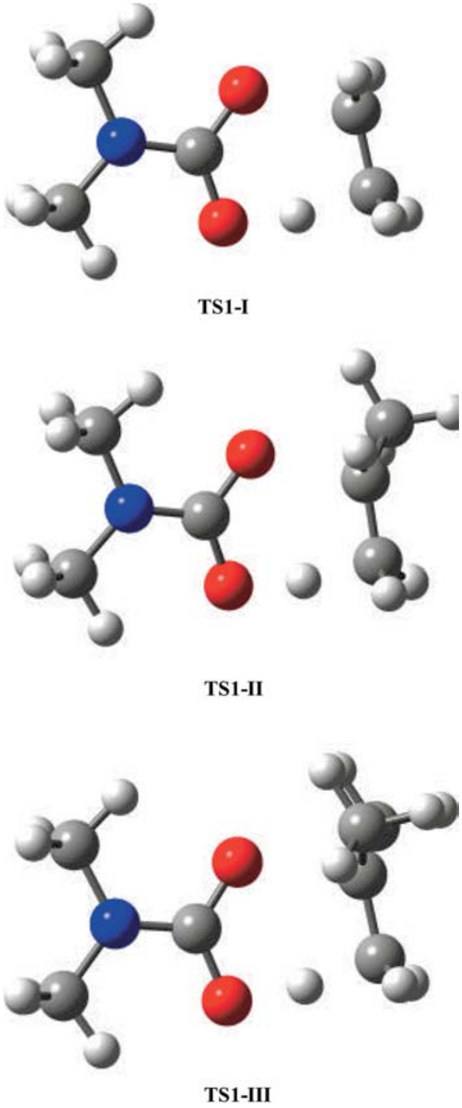
TS1-I

TS1-II

TS1-III

Fig. 5. Transition structures, optimized at the MP2/6-31G(d) level, for the first step of the thermolysis reaction of alkyl *N,N*-dimethylcarbamates

The geometries which were found for the TSs optimized at the MP2/6-31G(d) level are shown in Figs. 5, 6, and 7.

As an example of the IRC calculations done, the structures of the reactant and products of the first step of reaction IV, connected with the corresponding TS, TS1-IV, are shown in Fig. 8.

The results listed in Table 3 show the main distances for each optimized structure at the MP2/6-31G(d) and MP2/6-31++G(d,p) levels of theory. As can be observed, the geometrical parameters optimized at both theoretical levels are very similar. During the thermolysis process, when the reactant (dialkylcarbamate) is being transformed into its TS, the O_1–C_2, O_3–C_4, and C_5–H_6 distances increase, whereas the C_2–O_3, C_4–C_5, and H_6–O_1 distances decrease.

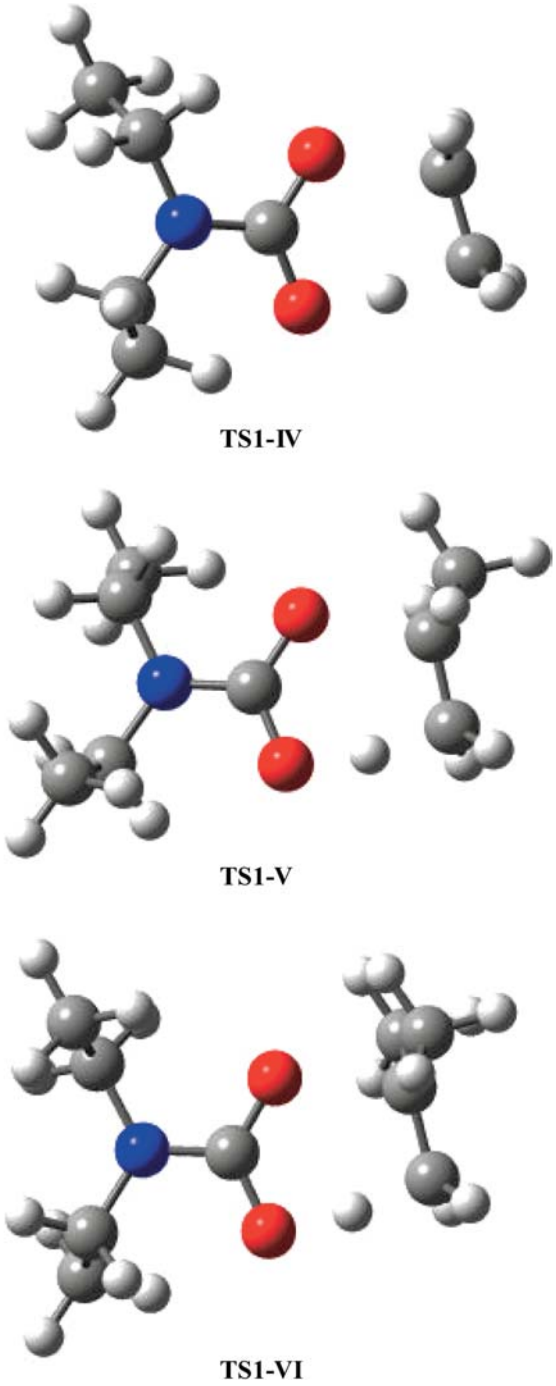
TS1-IV

TS1-V

TS1-VI

Fig. 6. Transition structures, optimized at the MP2/6-31G(d) level, for the first step of the thermolysis reaction of alkyl *N,N*–diethylcarbamates

The fundamental characteristics in this process are the O_3–C_4 (1.45–1.47 Å) and H_6–O_1 (2.37–2.71 Å) distances for each reactant. In the corresponding TS1s, the O_3–C_4 distance increases significantly (1.92–2.06 Å) by the breaking of this bond, while the H_6–O_1 distance decreases significantly (1.25–1.31 Å) by the formation of this bond.

The progress of the first step of the reactions has been followed by means of the Wiberg bond indices [19], B_i, defined as the sum of the squares of the off-diagonal density matrix elements between atoms. The bond index

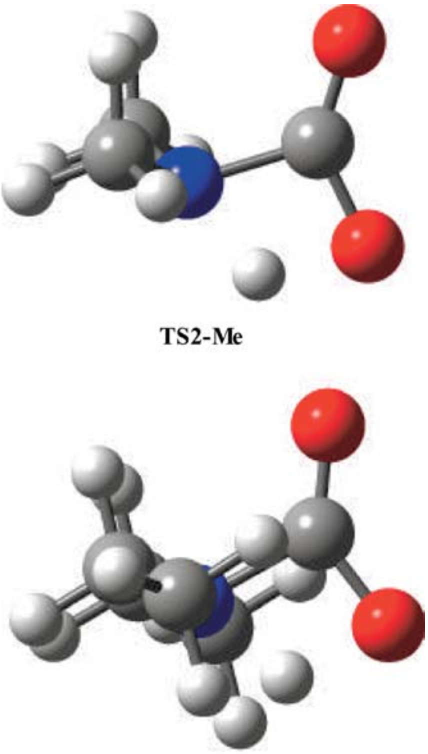

TS2-Me

TS2-Et

Fig. 7. Transition structures, optimized at the MP2/6-31G(d) level, for the decarboxylation. reaction of dialkylcarbamic acids

between two atoms is a measure of the bond order and, hence, of the bond strength between these two atoms. Thus, if the evolution of the bond indices corresponding to the bonds being made or broken in a chemical reaction is analyzed along the reaction path, a very precise image of the timing and extent of the bond-breaking and the bond-making processes at every point can be achieved [23]. The Wiberg bond indices corresponding to the bonds being made or broken in the reactions studied, for the reactants, TSs, and products, are collected in Table 4.

In order to perform the bond index analysis, it is convenient to define [23] a relative variation of the bond index at the TS, δB_i, for every bond, *i*, involved in a chemical reaction as

$$\delta B_i = \frac{\left(B_i^{\mathrm{TS}} - B_i^{\mathrm{R}}\right)}{\left(B_i^{\mathrm{P}} - B_i^{\mathrm{R}}\right)}, \tag{5}$$

where the superscripts R, TS, and P refer to reactants, TSs, and products, respectively.

The percentage of evolution of the bond order through the chemical step was calculated [24] by means of

$$\text{Percentage of evolution} = 100\delta B_i \tag{6}$$

and the values are collected in Table 4.

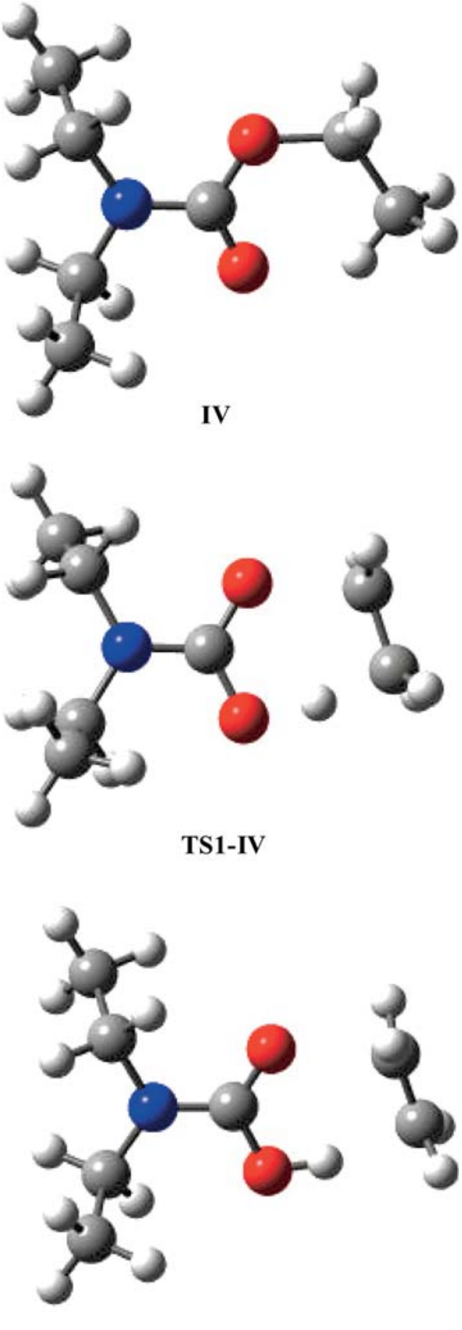

IV

TS1-IV

$(CH_3CH_2)_2NCOOH + CH_2{=}CH_2$

Fig. 8. Structures of reactant IV, transition state TS1-IV, and products, diethylcarbamic acid and ethylene of the first step of reaction IV, connected by an intrinsic reaction coordinate calculation

As can be observed in that table, the breaking of the O_3–C_4 bond is the most advanced process (58–60% in ethyl dialkylcarbamates, which increases to 69–70% in *tert*-butyl dialkylcarbamates), while the less advanced ones are the C_4–C_5 double-bond formation (only 31–32% in all the reactions) and the H_6 migration from C_5 to O_1 (41–42% in ethyl dialkylcarbamates, and only 35–36% in *tert*-butyl dialkylcarbamates)

Table 3. Main distances (angstroms) in the reactants, transition states, and products of the first step of the reactions, calculated at the MP2/6-31G(d) and MP2/6-31++G(d,p) levels. First value-obtained at the MP2/6-31G(d) level; second value obtained at theMP2/6-31++G(d,p) level

	O_1–C_2	C_2–O_3	O_3–C_4	C_4–C_5	C_5–H_6	H_6–O_1
I	1.228	1.367	1.447	1.515	1.091	2.670
	1.231	1.368	1.450	1.514	1.088	2.690
TS1-I	1.295	1.283	1.928	1.399	1.362	1.250
	1.296	1.288	1.921	1.403	1.342	1.255
$(CH_3)_2NCOOH$	1.372	1.227	–	–	–	0.977
	1.374	1.231				0.970
$CH_2=CH_2$	–	–	–	1.336	–	–
				1.339		
II	1.228	1.366	1.455	1.517	1.091	2.638
	1.231	1.367	1.458	1.517	1.088	2.696
TS1-II	1.294	1.281	1.990	1.401	1.336	1.277
	1.295	1.286	1.981	1.406	1.318	1.280
$CH_3CH=CH_2$	–	–	–	1.338	–	–
				1.341		
III	1.229	1.363	1.467	1.523	1.089	2.372
	1.232	1.364	1.471	1.523	1.087	2.388
TS1-III	1.292	1.280	2.055	1.406	1.313	1.304
	1.294	1.284	2.044	1.410	1.297	1.306
$(CH_3)_2C=CH_2$	–	–	–	1.341	–	–
				1.344		
IV	1.229	1.370	1.447	1.515	1.091	2.671
	1.233	1.372	1.450	1.514	1.088	2.702
TS1-IV	1.297	1.285	1.927	1.400	1.366	1.247
	1.299	1.290	1.917	1.404	1.348	1.249
$(CH_3CH_2)_2NCOOH$	1.374	1.229	–	–	–	0.977
	1.377	1.232				0.970
V	1.230	1.369	1.455	1.517	1.091	2.641
	1.233	1.371	1.457	1.517	1.089	2.706
TS1-V	1.295	1.284	1.988	1.402	1.339	1.275
	1.297	1.289	1.973	1.406	1.323	1.275
VI	1.231	1.367	1.467	1.523	1.090	2.375
	1.234	1.368	1.469	1.523	1.087	2.387
TS1-VI	1.295	1.282	2.051	1.406	1.318	1.300
	1.297	1.286	2.033	1.410	1.306	1.296

Table 4. Wiberg bond indices, B_i, of reactants, transition states, and products of the first step of the reactions, percentage of evolution (*%EV*) through the chemical process of the bond indices at the transition states, degree of advancement of the transition states, δB_{av}, and absolute synchronicities (*Sy*). Values calculated at the MP2/6-31G(d) and MP2/6-31++G(d,p) levels. First value obtained at the MP2/6-31G(d) level; second value obtained at the MP2/6-31++G(d,p) level

		O_1–C_2	C_2–O_3	O_3–C_4	C_4–C_5	C_5–H_6	H_6–O_1
Reaction I	B_i^{R}	1.588	0.959	0.833	1.029	0.928	0.001
		1.583	0.968	0.832	1.024	0.934	0.001
	B_i^{TS}	1.240	1.275	0.336	1.354	0.418	0.293
		1.250	1.270	0.346	1.334	0.444	0.283
	B_i^{P}	0.962	1.595	0.000	2.034	0.000	0.707
		0.970	1.590	0.000	2.035	0.000	0.699
	%EV	55.6	49.7	59.7	32.3	55.0	41.4
		54.3	48.6	58.4	30.7	52.5	40.4
	δB_{av}			0.490			
				0.475			
	Sy			0.901			
				0.900			
Reaction II	B_i^{R}	1.587	0.960	0.814	1.017	0.927	0.002
		1.582	0.969	0.816	1.014	0.933	0.001
	B_i^{TS}	1.246	1.286	0.285	1.331	0.440	0.275
		1.256	1.283	0.294	1.312	0.466	0.265
	B_i^{P}	0.962	1.595	0.000	1.985	0.000	0.707
		0.970	1.590	0.000	1.985	0.000	0.699
	%EV	54.6	51.3	65.0	32.4	52.5	38.7
		53.3	50.6	64.0	30.7	50.1	37.8
	δB_{av}			0.490			
				0.478			
	Sy			0.889			
				0.887			
Reaction III	B_i^{R}	1.580	0.965	0.799	1.004	0.920	0.003
		1.577	0.972	0.802	1.003	0.925	0.002
	B_i^{TS}	1.257	1.294	0.240	1.299	0.462	0.256
		1.265	1.293	0.247	1.284	0.486	0.247
	B_i^{P}	0.962	1.595	0.000	1.934	0.000	0.707
		0.970	1.590	0.000	1.931	0.000	0.699
	%EV	52.3	52.2	70.0	31.7	49.8	35.9
		51.4	51.9	69.2	30.3	47.5	35.2
	δB_{av}			0.487			
				0.476			
	Sy			0.878			
				0.875			
Reaction IV	B_i^{R}	1.578	0.953	0.835	1.029	0.928	0.001
		1.566	0.959	0.834	1.024	0.934	0.001
	B_i^{TS}	1.232	1.271	0.338	1.355	0.413	0.296
		1.237	1.259	0.351	1.335	0.438	0.288
	B_i^{P}	0.958	1.587	0.000	2.034	0.000	0.708
		0.964	1.575	0.000	2.035	0.000	0.700
	%EV	55.8	50.2	59.5	32.4	55.5	41.7
		54.7	48.7	57.9	30.8	53.1	41.1
	δB_{av}			0.492			
				0.477			
	Sy			0.901			
				0.901			
Reaction V	B_i^{R}	1.576	0.954	0.815	1.017	0.928	0.002
		1.565	0.960	0.819	1.014	0.933	0.001
	B_i^{TS}	1.241	1.279	0.288	1.330	0.438	0.277
		1.245	1.269	0.301	1.311	0.463	0.269
	B_i^{P}	0.958	1.587	0.000	1.985	0.000	0.708
		0.964	1.575	0.000	1.985	0.000	0.700
	%EV	54.2	51.3	64.7	32.3	52.8	39.0
		53.2	50.2	63.2	30.6	50.4	38.3
	δB_{av}			0.491			
				0.477			
	Sy			0.891			
				0.890			

The elongation of the O_3–C_4 bond with the migration of the H_6 atom from C_5 to O_1 can be seen as the driving force for the reaction studied.

The average value, δB_{av}, calculated [23] as

$$\delta B_{av} = \frac{1}{n}\sum \delta B_i \tag{7}$$

where n is the number of bonds involved in the reaction, affords a measure of the degree of advancement of the TS along the reaction path. Calculated δB_{av} values for the studied reactions are shown in Table 4. As can be seen in this table, the δB_{av} values, 0.49 in all the cases, show that the TSs have character intermediate between the reactants and the products.

One can also obtain information on the absolute asynchronicity, A, of a chemical reaction using the expression proposed by Moyano et al. [23]:

$$A = \frac{1}{(2N-2)}\sum \frac{|\delta B_i - \delta B_{av}|}{\delta B_{av}}. \tag{8}$$

Table 4. (Contd.)

		O_1–C_2	C_2–O_3	O_3–C_4	C_4–C_5	C_5–H_6	H_6–O_1
Reaction VI	B_i^R	1.568	0.958	0.801	1.004	0.920	0.003
		1.559	0.963	0.804	1.003	0.925	0.002
	B_i^{TS}	1.248	1.288	0.242	1.300	0.457	0.259
		1.250	1.280	0.254	1.287	0.477	0.255
	B_i^P	0.958	1.587	0.000	1.934	0.000	0.708
		0.964	1.575	0.000	1.931	0.000	0.700
	%EV	52.5	52.5	69.8	31.8	50.3	36.3
		51.9	51.8	68.4	30.6	48.4	36.2
	δB_{av}			0.489			
				0.479			
	Sy			0.879			
				0.879			

The opposite of the asynchronicity, the synchronicity, Sy, defined as

$$\mathrm{Sy} = 1 - A \tag{9}$$

varies between zero, when one of the n bonds has completely broken at the TS while the other n–1 bonds remain completely unchanged, and unity, when all the n bonds have broken or formed to exactly the same extent in the TS.

The Sy values obtained in this way are, in principle, independent of the degree of advancement of the TS. The Sy values calculated for the reactions studied are shown in Table 4. As can be seen in that table, the synchronicities are 0.90 for ethyl dialkylcarbamates, and the values decrease to 0.88 for *tert*-butyl dialkylcarbamates, indicating that the mechanisms correspond to slightly asynchronous processes; the asynchronicity increases from ethyl to *tert*-butyl derivatives.

A last aspect to be taken into account is the relative asynchronicity of the bond-breaking and the bond-forming processes that it would be a measure of "bond deficiency" along the reaction path. In the reactions studied, the bond-breaking processes are clearly more advanced (an average of 55–57%) than the bond-forming ones (an average of 39–41%), indicating a bond deficiency in the TSs.

The charge distribution in reactants and TSs was analyzed by means of the NBO analysis of Reed and Weinhold [17, 18]. We have collected the natural atomic charges (the nuclear charges minus the summed natural populations of the natural atomic orbitals on the atoms) at the atoms involved in the reaction in Table 5.

Table 5. Natural bond order charges, calculated at the MP2/6-31G(d) and MP2/6-31++G(d,p) levels, at the atoms involved in the reaction center, for reactants and transition states of the first step of the reactions. First value obtained at the MP2/6-31G(d) level; second value obtained at the MP2/6-31++G(d,p) level

	O_1	C_2	O_3	C_4	C_5	H_6
I	−0.776	1.145	−0.674	−0.040	−0.672	0.238
	−0.776	1.135	−0.676	−0.030	−0.639	0.230
TS1-I	−0.843	1.171	−0.802	0.022	−0.886	0.479
	−0.835	1.153	−0.800	0.046	−0.867	0.462
II	−0.776	1.150	−0.683	0.143	−0.665	0.242
	−0.776	1.138	−0.685	0.127	−0.629	0.212
TS1-II	−0.847	1.168	−0.824	0.223	−0.867	0.472
	−0.840	1.150	−0.822	0.240	−0.848	0.455
III	−0.781	1.153	−0.688	0.330	−0.666	0.254
	−0.780	1.144	−0.692	0.301	−0.632	0.246
TS1-III	−0.853	1.167	−0.844	0.424	−0.854	0.468
	−0.847	1.149	−0.844	0.452	−0.839	0.452
IV	−0.782	1.144	−0.675	−0.040	−0.672	0.237
	−0.785	1.137	−0.680	−0.029	−0.638	0.229
TS1-IV	−0.845	1.170	−0.803	0.021	−0.888	0.480
	−0.839	1.154	−0.802	0.043	−0.869	0.464
V	−0.782	1.148	−0.685	0.143	−0.665	0.242
	−0.785	1.140	−0.689	0.129	−0.628	0.232
TS1-V	−0.848	1.166	−0.826	0.223	−0.869	0.472
	−0.844	1.151	−0.825	0.238	−0.850	0.456
VI	−0.787	1.151	−0.690	0.330	−0.665	0.254
	−0.790	1.146	−0.697	0.302	−0.631	0.247
TS1-VI	−0.855	1.166	−0.845	0.422	−0.855	0.470
	−0.851	1.150	−0.846	0.446	−0.841	0.455

Charges at TS1s show an important positive charge developed on H_6 (0.45–0.48 at TS1s and 0.21–0.25 at reactants), while the electronic excess is supported by the two oxygens (−0.84 to –0.86 at TS1s and −0.78 to −0.79 at reactants, for O_1, and –0.80 to –0.85 at TS1s and −0.67 to −0.69 at reactants, for O_3) and by C_5 (−0.84 to −0.89 at TS1s and −0.63 to −0.67 at reactants). The negative character of O_1 allows it to attract the H_6 in the TS. The same hydrogen atom has a more positive character in the TS1s and thus O_1 increases its negative character, and C_5 has a more negative character, as would be expected by the postulated cyclic TS.

The most significant difference among the alkyl carbamates is the charge at atom C_4. This charge is significantly more positive going from the ethyl to the *tert*-butyl derivative. This is owing to the electron-withdrawing effect of the methyl groups attached to atom C_4.

The calculated kinetic and activation parameters for the reactions studied are shown in Table 6 and are compared with the available experimental results. They were calculated at the same temperature used in the experiments, 593.15 K. As can be seen, the computed values, at the MP2/6-311++G(2d,p)//MP2/6-31G(d) level of theory, agree well with the experimental data, the rate constants and activation free energies being very close to the experimental values. However, the agreement between experimental and calculated activation entropies is very bad. This fact is difficult to explain and perhaps the good agreement between the k and $\Delta G^{\neq}$ values in spite of the disagreement in the $\Delta S^{\neq}$ values is due to error cancellation. Similar behavior has been previously observed by us in studies of the thermolysis in the gas phase of ethyl β-hydroxycarboxylates [25], and α-amino acid ethyl esters [26, 27], at similar theoretical levels.

As can be observed, the order of reactivity, tertiary > secondary > primary alkyl ester, is the same in both series, *N*,*N*-dimethylcarbamates and *N*,*N*-diethylcarbamates. This sequence is to be expected from electron release to the reaction center, where the elongation of the O_3–C_4 bond and polarization in the sense $O_3{}^{\delta-}\cdots C_4{}^{\delta+}$ is the rate-determining step of these reactions. The O_3–C_4

Table 6. Theoretical [evaluated at the MP2/6-311+ +G(2d,p)//MP2/6-31G(d) level; values in *parentheses* are those calculated at the MP2/6-31+ +G(d,p) level] and experimental (values for reactions I, II, and III, taken from Ref. [6], except the values in *brackets* for reaction III, taken from Ref. [7]; values for reactions IV,V, and VI, taken from Ref. [8]) kinetic and activation parameters for the pyrolysis of*N*,*N*-dimethyldiethylcarbamates and *N*,*N*-diethylcarbamates, at 593.15 K

Reaction	10^4k (s^{-1})		E_a (kJ mol^{-1})		log*A*		$\Delta H^{\neq}$ (kJ mol^{-1})		$\Delta G^{\neq}$ (kJ mol^{-1})		$\Delta S^{\neq}$ (J mol^{-1} K^{-1})	
	Calc	Exp	Calc	Exp	Calc	Exp	Calc	Exp	Calc	Exp	Calc	Exp
I	1.8 (0.43)	0.58	198.4 (205.5)	185.5	13.7	12.10	193.5 (200.6)	180.6	191.1 (198.2)	196.7	4.0	−27.2
II	8.0 (1.8)	12.02	190.9 (198.2)	181.2	13.7	13.04	186.0 (193.3)	176.3	183.8 (191.2)	181.8	3.6	−9.2
III	763 (160)	912.0 [782.2]	174.1 (181.7)	157.9 [163.2]	14.2	12.87 [13.27]	169.2 (176.8)	153.0 [158.3]	161.3 (169.0)	160.3 [161.2]	13.2	−12.3 [−4.9]
IV	1.0 (0.26)	0.56	198.7 (205.4)	178.4 ± 3.1	13.5	11.47 ± 0.25	193.8 (200.5)	173.5	193.9 (200.6)	196.8	−0.2	-39.3
V	5.0 (1.2)	9.77	191.9 (198.9)	179.8 ± 7.9	13.6	12.83 ± 0.70	187.0 (194.0)	174.9	186.1 (193.0)	182.8	1.6	−13.3
VI	576(128)	794.3	175.5(182.8)	158.6 ± 6.2	14.2	12.87 ± 0.62	170.6(177.9)	153.7	162.7(170.1)	161.1	13.2	−12.5

distance in TS1s (Table 3), the charge difference between both atoms (Table 5), and the percentage of evolution of the $O_3{-}C_4$ bond (Table 4) significantly increase in the order ethyl < isopropyl < *tert*-butyl carbamate. Comparing *N*,*N*-dimethyllcarbamates with *N*,*N*-diethylcarbamates, the $(CH_3CH_2)_2N$ substituent at the acid side of the ester tends to decrease the rate slightly compared with the $(CH_3)_2N$ group. This difference may be rationalized in terms of the greater electron-releasing power of the CH_3CH_2 group to the N atom than CH_3. This reduces the electron-withdrawing effect of the diethylamino group and a slight decrease in the rate of elimination results [8].

The second step of the reactions, corresponding to the decarboxylation of the dialkylcarbamic acid intermediates, occurs via a four-membered cyclic TS (TS2s). It is a rapider process than the first step of the reactions, with activation energies of 144.1 and 140.0 kJ mol^{-1} for the decarboxylation process of dimethylcarbamic and diethylcarbamic acid, respectively, and with calculated rate constants of 0.80 and 3.60 s^{-1}, respectively, evaluated at the MP2/6-311+ +G(2d,p)//MP2/6-31G(d) level of theory.

Conclusions

A theoretical study on the thermal decomposition in the gas phase of several alkyl *N*,*N*-dialkylcarbamates has been carried out in order to explore the nature of the reaction mechanism.

The decomposition process in the gas phase of the carbamates studied occurs in two steps: the first one, the rate-determining step, is a concerted process in which an alkene and a dialkylcarbamic acid intermediate are formed, via a six-membered cyclic TS; the second one, the decarboxylation of the intermediate, occurs via a four-membered cyclic TS, leading to CO_2 and the corresponding dialkylamine, as is shown by the free-energy profiles.

The progress of the reactions was followed by means of the Wiberg bond indices. The lengthening of the $O_3{-}C_4$ bond with the migration of the H_6 atom from C_5 to O_1 can be seen as the driving force for the reactions studied. The TSs have character intermediate between reactants and products. The calculated synchronicities show that the reactions are slightly asynchronous; the asynchronicity increases in the order ethyl < isopropyl < *tert*-butyl derivative. The bond-breaking processes are more advanced than the bond-forming ones, indicating a bond deficiency in the TSs.

The rate constants and activation free energies for the reactions studied, evaluated at the MP2/6-311+ +G(2d,p)//MP2/6-31G(d) level of theory, agree very well with the available experimental data.

Acknowledgements. This work was supported by a research fund provided by the Comité de Investigación y Desarrollo Científico, Universidad Nacional de Colombia, Sede Medellín, and COLCIENCIAS (project no. 1118-05-1148), and the Spanish Dirección

General de Investigación, Ministerio de Ciencia y Tecnología (project no. BQU20001499). The authors also thank COLCIENCIAS and C.S.I.C. for the joint project no. 2001CO0004, and the program Formación de Jóvenes Investigadores (Ederley Vélez)—COLCIENCIAS.

References

1. Daly NJ, Ziolkowski F (1971) Aust J Chem 24:2451
2. Smith GG, Voorkees KJ, Kelly FM (1971) J Chem Soc Chem Commun 789
3. Gordon AS, Norris WP (1965) J Phys Chem 69:3013
4. Kwart H, Slutsky J (1972) J Chem Soc Chem Commun 552
5. Daly NJ, Ziolkowski F (1972) Aust J Chem 25:1453
6. Daly NJ, Ziolkowski F (1972) J Chem Soc Chem Commun 911
7. Kwart H, Slutsky J (1972) J Chem Soc Chem Commun 1182
8. Herize A, Domínguez RM, Rotinov A, Núñez O, Chuchani G (1999) J Phys Org Chem 12:201
9. Chuchani G, Mishima M, Notario R, Abboud JLM (1999) In: Charton M, Charton BI (eds) Advances in quantitative structure-property relationships, vol 2. JAI, Stamford, p 35
10. Frisch MJ, Trucks GW, Schlegel HB, Scuseria GE, Robb MA, Cheeseman JR, Zakrzewski VG, Montgomery JA Jr, Stratmann RE, Burant JC, Dapprich S, Millam JM, Daniels AD, Kudin KN, Strain MC, Farkas O, Tomasi J, Barone V, Cossi M, Cammi R, Mennucci B, Pomelli C, Adamo C, Clifford S, Ochterski J, Petersson GA, Ayala PY, Cui Q, Morokuma K, Salvador P, Dannenberg JJ, Malick DK, Rabuck AD, Raghavachari K, Foresman JB, Cioslowski J, Ortiz JV, Baboul AG, Stefanov BB, Liu G, Liashenko A, Piskorz P, Komaromi I, Gomperts R, Martin RL, Fox DJ, Keith T, Al-Laham MA, Peng CY, Nanayakkara A, Challacombe M, Gill PMW, Johnson B, Chen W, Wong MW, Andrés JL, González C, Head-Gordon M, Replogle ES, Pople JA, (2001) Gaussian 98, revision A.11.3. Gaussian, Pittsburgh, PA
11. Møller C, Plesset M (1934) Phys Rev 46:618
12. Ditchfield R, Hehre WJ, Pople JA (1971) J Chem Phys 54:724
13. Scott PA, Radom L (1996) J Phys Chem 100:16502
14. McQuarrie DA, Simon JD (1999) Molecular thermodynamics. University Science Books, Sausalito, CA
15. Fukui K (1970) J Phys Chem 74:4161
16. Clark T, Chandrasekhar J, Spitznagel GW, Schleyer PvR (1983) J Comput Chem 4:294
17. Reed AE, Weinhold F (1983) J Chem Phys 78:4066
18. Reed AE, Curtiss LA, Weinhold F (1988) Chem Rev 88:899
19. Wiberg KB (1968) Tetrahedron 24:1083
20. Glendening ED, Reed AE, Carpenter JE, Weinhold F NBO, version 3.1, Madison, WI, 1988.
21. Glasstone KJ, Laidler KJ, Eyring H (1941) The theory of rate processes. McGraw–Hill, New York, chap 4
22. Benson SW (1969) The foundations of chemical kinetics. McGraw–Hill, New York
23. Moyano A, Pericàs MA, Valentí E (1989) J Org Chem 54:573
24. Domingo LR, Picher MT, Safont VS, Andrés J, Chuchani G (1999) J Phys Chem A 103:3935
25. Notario R, Quijano J, Quijano JC, Gutiérrez LP, Suárez WA, Sánchez C, León LA, Chamorro E (2002) J Phys Chem A 106:4377
26. Quijano J, Notario R, Chamorro E, León LA, Sánchez C, Alarcón G, Quijano JC, Chuchani G (2002) J Phys Org Chem 15:413
27. Notario R, Quijano J, León LA, Sánchez C, Quijano JC, Alarcón G, Chamorro E, Chuchani G (2003) J Phys Org Chem 16:166